FcRL4 acts as an adaptive to innate molecular switch dampening BCR signaling and enhancing TLR signaling

Hae Won Sohn,[1] Peter D. Krueger,[1] Randall S. Davis,[2] and Susan K. Pierce[1]

[1]Laboratory of Immunogenetics, National Institute of Allergy and Infectious Diseases, National Institutes of Health, Rockville, MD; and [2]Department of Medicine, Microbiology, Molecular Genetics and Biochemistry, University of Alabama at Birmingham, Birmingham, AL

Fc receptor–like 4 (FcRL4) is expressed on the surface of a subset of memory B cells (MBCs) located at sites of invading pathogens in mucosal lymphoid tissues in healthy individuals. Recently, FcRL4+ MBCs were shown to be greatly increased in number in the peripheral blood of HIV-infected viremic individuals, in whom they are associated with B-cell exhaustion, and in individuals chronically reinfected with malaria. In the present study, we provide evidence that the expression of FcRL4 in human B-cell lines disrupts immune synapse formation and blocks antigen-induced BCR signaling at the point of Syk phosphorylation, blocking downstream activation of PLC-γ2 and Vav and the induction of calcium responses and CD69 expression. FcRL4 functions by ligation-independent mechanisms that require the 3 tyrosine residues in its cytoplasmic domain and involves its phosphorylation and association with the tyrosine phosphatases SHP-1 and SHP-2. Remarkably, FcRL4 is concentrated in endosomes after treatment with the TLR9 agonist CpG and enhances signaling through TLR9, as measured by increased expression of CD23. These findings suggest that FcRL4 may act as a molecular switch in B cells to dampen adaptive immune signaling and enhance innate signaling in response to chronic antigenic stimulation. (*Blood*. 2011;118(24): 6332-6341)

Introduction

Fc receptor–like (FcRL) proteins are an ancient multigene family of transmembrane proteins that share ancestors with the classic FcRs and are preferentially expressed in the B-cell lineage.[1] Despite their sequence similarity with classic FcRs, the FcRLs do not bind Igs and, with the exception of FcRL6, a receptor selectively expressed on cytotoxic T cells and natural killer cells that binds HLA-DR,[2] ligands of the FcRLs have not been identified. The absence of known ligands leaves open the possibility that FcRLs may function constitutively, independently of ligation. The immunoregulatory potential of the FcRLs is suggested by the presence of immunoreceptor tyrosine–based inhibitory motifs (ITIMs) and switch motifs in their cytoplasmic domains.

Ehrhardt et al first described FcRL4 to mark a unique population of memory B cells (MBCs) in human lymphoid tissues near epithelial surfaces that had distinctive functional capabilities.[3] In humans, FcRL4+ MBCs lack CD27, the classic marker for MBCs, and, compared with FcRL4− MBCs, express more CD20 and less CD21 and have strongly up-regulated CCR1 and CCR5 that may play a role in their tissue localization. FcRL4+ and FcRL4− MBCs have undergone isotype switching and somatic hypermutation to similar levels, but neither expresses transcription factors associated with plasma-cell differentiation. FcRL4+ MBCs do not proliferate in response to BCR cross-linking, but differentiate into plasma cells in response to IL-2, IL-10, and CD40 ligand. These results suggest that FcRL4+ MBCs have dampened signaling through the BCR while maintaining their sensitivity to cytokines and T-cell help. Subsequent comparative transcriptome and proteome analyses revealed that FcRL4+ and FcRL4− MBCs had distinctive expression of a variety of genes providing a signature for FcRL4+ MBCs,[4] including genes encoding: (1) cell-surface markers, including CD11c, CCR1, CCR5, RANKL, and DLL1; (2) regulators of the cell cycle; (3) signal-transduction molecules such as FgR and Hck; and (4) transcription factors, including RUNX2 and SOX5. The investigators of that study concluded that these distinctive MBCs residing in close proximity to epithelial tissues in mucosal lymphoid tissues may play an important role in healthy individuals in humoral immune responses at epithelial boundaries in the body in close proximity to the natural microflora and sites of invading pathogens.

Moir et al described a similar population of FcRL4+ MBCs in the peripheral blood of HIV-infected viremic individuals.[5] Compared with FcRL4− MBCs, these FcRL4+ MBCs expressed high levels of inhibitory receptors, including CD22 and CD85j. The profile of trafficking receptors was similar to that described for FcRL4+ MBCs in tissues by Ehrhardt et al,[3,4] suggesting that these FcRL4+ MBCs in the blood of HIV-viremic individuals were migrating from lymphoid tissues to chronically inflamed tissues. Compared with FcRL4− MBCs, FcRL4+ MBCs from HIV-viremic individuals showed reduced proliferation and differentiation into plasma cells in response to the cytokines IL-2 and IL-10, T-cell help in the form of CD40L, and BCR cross-linking.[5] Because the pattern of expression of inhibitory and homing receptors by FcRL4+ MBCs in HIV-viremic individuals was similar to that described for virus-specific CD8+ T-cell exhaustion in chronic lymphocytic choriomeningitis virus infections in mice and in HIV-viremic individuals,[6-8] Moir et al called these FcRL4+ MBCs "exhausted MBCs."[5,9] HIV-specific B cells were enriched in the FcRL4+ MBC population, in contrast to influenza-specific B cells, which were concentrated in the FcRL4− MBC population,[5] suggesting that exhaustion of MBCs was antigen driven and may

contribute to the poor antibody responses in HIV-infected individuals.

We subsequently showed that FcRL4+ MBCs were greatly increased in number in the peripheral blood of children and adults living in Mali, a malaria-endemic area of Africa where malaria transmission is both intense and seasonal.[10] We found that in children as young as 2 years of age, the FcRL4+ MBC population represented up to 30% of their circulating B cells. The number of FcRL4+ MBCs was highest in children with chronic asymptomatic *Plasmodium falciparum* infections during long periods of no malaria transmission, suggesting the possibility that the chronic presence of the parasite drives the expansion of FcRL4+ MBCs in the peripheral circulation.

The cytoplasmic tail of FcRL4 contains a switch motif and 2 ITIMs that have been shown to inhibit BCR signaling when expressed in a chimeric protein containing the ectomembrane and transmembrane domains of FcγRIIB and the cytoplasmic domain of FcRL4.[11] In these studies, inhibition required co-ligation of the BCR and the FcγRIIB-FcRL4 chimera, and involved the phosphorylation of both ITIM tyrosines in the FcRL4 tail and recruitment of the tyrosine phosphatases SHP-1 and SHP-2. Although these results clearly demonstrate the inhibitory potential of the FcRL4 cytoplasmic domain, because FcRL4 does not bind Ig or immune complexes and consequently may not have a means to be co-ligated to the BCR, it is not known if or how FcRL4 expressed in human B cells can regulate BCR signaling. Recently, silencing of FcRL4 in tissue-like MBCs from HIV-viremic individuals was shown to restore BCR-induced proliferation,[12] providing direct evidence for a role of FcRL4 in B-cell exhaustion. In the present study, we provide evidence that the expression of FcRL4 in human B-cell lines results in the inhibition of BCR signaling independently of FcRL4-BCR co-ligation at the point of Syk phosphorylation by a mechanism that involves phosphorylation of FcRL4 and its association with SHP-1 and SHP-2. We also show that FcRL4 expression simultaneously enhances responses to the TLR9 agonist CpG, suggesting that FcRL4 may function to switch B-cell responsiveness from adaptive BCR-mediated signaling to innate TLR-receptor signaling.

Methods

Cell lines, antibodies, and reagents

Ramos cells (R2G6), a human Burkitt lymphoma cell line, were maintained in RPMI medium supplemented with 10% FBS, Pen/Strep, 2mM L-glutamine, 10mM HEPES, and 55 μM β-mercaptoethanol (Invitrogen). Human B cells from PBMCs of healthy donors were purified using the MACS B-cell negative isolation kit (Miltenyi Biotech), frozen in 10% DMSO, and kept in liquid nitrogen until use. Cy3- or DyLight649-goat Fab anti–human IgM (heavy chain specific), biotinylated goat Fab anti–human IgM, and goat F(ab′)$_2$ anti-IgG + IgM (H+L) were purchased from Jackson ImmunoResearch Laboratories. The APC-conjugated mouse mAbs specific for human IgM, PE- or APC-conjugated mouse mAb anti–human CD69, PE mouse mAb specific for human CD23 (BD Biosciences) and PE-conjugated mouse mAb specific for human FcRL4 (BioLegend) were used for FACS analyses. Calcium dyes, Fluo4-NW, and Fura Red were from Invitrogen. Recombinant human ICAM-1/human Fc chimera protein (R&D Systems) was biotinylated using NHS-LC-Biotin (Thermo Scientific) as described previously.[13] CpG oligodeoxynucleotide (ODN) 2006 (type B) and control ODNs were from InvivoGen. Mouse mAb anti–human TLR9 was from Imgenex. For imaging or sorting FcRL4+ cells, mouse mAb anti–human FcRL4 (clone 10E6) was conjugated with Alexa Fluor 647 following the manufacturer's protocol (Invitrogen). Mouse mAb and rabbit Abs anti-GFP (Invitrogen), goat Abs anti–human FcRL4 (R&D), rabbit Abs

anti-Igβ, Syk, Vav, PLC-γ2, and SHP-1 (Santa Cruz Biotechnology), and mouse mAb anti–SHP-2 (BD Biosciences) were used for immunoprecipitation and immunoblotting, with the exception of SHP-1 and SHP-2, in which mouse mAb anti–SHP-1 (BD Biosciences) and rabbit Abs anti–SHP-2 were used for immunoblotting. The phospho-tyrosine specific mouse mAb 4G10 conjugated to HRP (4G10-HRP; Millipore) was used for the detection of tyrosine-phosphorylated proteins.

Plasmids, transient and stable transfections

A plasmid expressing the human FcRL4-yellow fluorescent protein (FcRL4-YFP) fusion protein was constructed by the insertion of human FcRL4, a kind gift of Dr Satoshi Nagata (Sanford Research/University of South Dakota, Sioux Falls, SD) into the pEYFP-N1 vector (Clontech)[14] through the *Hin*dIII and AgeI sites, resulting in a 5–amino acid linker between FcRL4 and YFP. The mutations of the cytoplasmic domain tyrosines to phenylalanines of the FcRL4 at positions 451 (Y451F), 463 (Y463F), and 493 (Y493F) and all 3 tyrosines (FFF) were generated with the Quick-Change II XL Site-directed Mutagenesis kit (Stratagene) as described previously.[15] All mutations were confirmed by sequencing (Macrogen-nUSA). For the establishment of stable Ramos cell lines expressing FcRL4-YFP or FcRL4 with tyrosine-mutated or wild-type cytoplasmic domains, cells were electroporated at 960 μF and 300 V (Bio-Rad),[16] selected with antibiotics, and sorted after staining with a mouse mAb anti-FcRL4 (10E6) to obtain the cells expressing FcRL4 on the surface. The transient transfection of human primary B cells with YFP or FcRL4-YFP plasmid was performed using the Amaxa human B-cell nucleofector kit (Lonza).

Preparation of PLBs and live cell imaging

Planar lipid bilayers (PLBs) containing human ICAM-1/huFc, and goat F(ab′)$_2$ or Fab anti–human IgM, were prepared as described previously[13,17] on an 8-well Lab-Tek chambered coverglass (Nalge Nunc) and the chambers were filled with 400 μL of 1% BSA-PBS immediately before imaging. Total internal reflection fluorescence (TIRF) microscopy for live-cell image acquisition was carried out as described previously.[18] Briefly, an IX-81 microscope equipped with a total internal reflection (TIR) illumination port, a 100 × 1.45 numerical aperture, oil-immersion objectives (Olympus) and a 512 × 512 pixel electron-multiplying charge-coupled device camera, Cascade II (Roper Industries) were controlled by Metamorph software (MDS Analytical Technologies) for image acquisition. For 2-color images, Ex514 nm/Em 550/40 ET/BP for YFP or Cy3, and Ex647 nm/Em665LP for DyLight649 or Alexa Fluor 647 were used to obtain either YFP-DyLight649 or Cy3–Alexa Fluor 647 images. Two-color, time-lapse, live-cell TIRF images for YFP and DyLight649 were acquired at 37°C on a heated chamber by switching the laser and emission filter from 514 to 647 using multiple dimensional acquisition mode controlled by Metamorph with a 2-second interval after adding cells into chambers with PLB. The TIR angle, controlled by MS2000 automated X-Y, piezo Z stage (ASI), was predetermined and fine-tuned for each experiment. For epifluorescence imaging, images were obtained at the same condition except for the TIR angle zero. For image processing, we mainly used Image Pro Plus (IPP; Media Cybernetics) except for the co-localization analysis using ImageJ software (available at http://rsbweb.nih.gov/ij/). For the analysis of normalized mean fluorescence intensity (NMFI) over the cell contact area, time-lapse TIRF images for the BCR were first subtracted with MFI from the surrounding background of the cell's contacted area and then the region of interest at the maximum contact area of each cell was applied to the all time frames to obtain MFI by the intensity track option in IPP. Acquired intensity data from multiple cells were analyzed in Excel and normalized by the MFI of the surface BCR in each cell obtained from background subtracted epifluorescence images. For the co-localization analysis between the BCR and FcRL4 in fixed cells or with time after B cells contacted the Ag-bound PLB, the Pearson co-localization coefficient (Rr) was calculated using WCIF-ImageJ according to the online manual from a set of FcRL4 and IgM images. Background-subtracted images were applied to the calculation of Rr on the basis of intensity correlation analysis. For co-localization analysis of FcRL4 and CpG, 2-color confocal imaging was

performed using a Zeiss LSM 510 Meta microscope equipped with a 1.4 oil plan-apochromat ×63 objective as described previously,[19] and the images were processed using ZEN 2009 software (Carl Zeiss). FcRL4-YFP and CpG-Cy3 images were sequentially acquired with Ex488/Em505-550BP and Ex543/Em560-615BP, respectively.

Immunoprecipitation and immunoblotting

Immunoprecipitation and immunoblotting were as described previously.[20] In brief, cells (1×10^7/mL) were pre-incubated with serum-free RPMI medium supplemented with 10mM HEPES at 37°C for 3 hours and resuspended at 5×10^7 cells/mL of fresh serum-free medium and stimulated with goat F(ab′)$_2$ anti–human IgM or species-matched control IgG at 37°C. Cells were lysed with 1% NP-40 (Calbiochem) lysis buffer, precleared with protein G magnetic beads (Invitrogen), and immunoprecipitated with either control- or specific antibody–bound protein G magnetic beads at 4°C overnight. To quantify the phosphorylation of the immunoprecipitated proteins, immunoblots were first probed with 4G10-HRP, then the probes were stripped, and the blots were reprobed with antibodies specific for the proteins.

Measurement of intracellular Ca²⁺ flux

Measurement of Ca^{2+} flux was as described previously.[21] Briefly, cells (5×10^6/mL) were loaded with Fluo-4 provided with the Fluo-4 NW assay kit at 37°C for 30 minutes following the manufacturer's protocol (Invitrogen). Fura Red was directly added to the HBSS containing Fluo-4NW, resulting in a final concentration of 5.0 μg/mL. Cells were resuspended in HBSS containing 1% BSA at 1×10^7/mL and 1×10^7 cells were analyzed using a FACSCalibur (BD Biosciences). Changes of fluorescence intensities of Fluo-4 and Fura Red were recorded for 512 seconds. After a 30-second baseline recording, 20 μg/mL of F(ab′)$_2$ anti-Ig was added.

Statistical analyses

All repeated or multiple sample data were analyzed by Student t test using either Prism 5 (GraphPad) or SigmaPlot 10 (Systat) software.

Results

Spatial distribution of FcRL4 and the BCR during immune synapse formation

To investigate the effect of FcRL4 expression in human B cells, constructs encoding FcRL4 containing YFP at the C terminus were transfected into human FcRL4⁻ Ramos B cells. The levels of expression of the BCR were similar in FcRL4⁺ and FcRL4⁻ B cells (Figure 1A), and in FcRL4⁺ cells, the BCR and FcRL4 at the B-cell surface appeared to be uniformly distributed (Figure 1B). In addition, a portion of FcRL4 was present in intracellular compartments (Figure 1B). To investigate the response of FcRL4⁺ and FcRL4⁻ B cells to BCR ligation, cells were placed on fluid lipid bilayers containing lipid-anchored Fab goat Abs specific for human IgM (Fab anti-IgM). Using TIRF microscopy, we observed that FcRL4⁻ B cells rapidly accumulated BCR in the contact area between the cell and the lipid bilayer and ultimately formed an immune synapse (IS), with the BCR concentrated at the center of the contact area of the cell with the bilayer; this was consistent with our previous studies in mouse B cells (Figure 2A-B and supplemental Video 1, available on the *Blood* Web site; see the Supplemental Materials link at the top of the online article).[13,18] Compared with FcRL4⁻ B cells, FcRL4⁺ B cells accumulated BCRs at the interface of the cell and the lipid bilayer to lower levels (Figure 2A-B and supplemental Video 2). After 18-24 hours on the bilayers, fewer FcRL4⁺ cells (31.0%) expressed the activation marker CD69 compared with FcRL4⁻ cells (57.1%; supplemental Figure 1). In
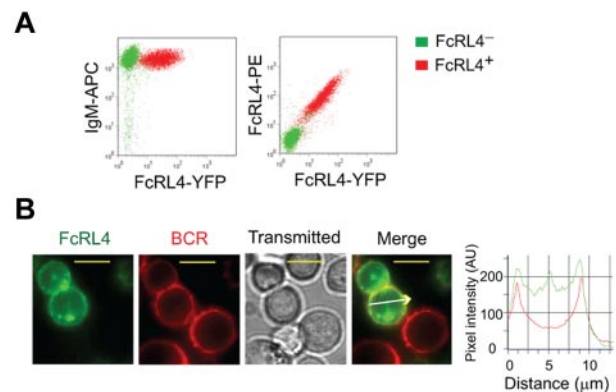

Figure 1. Expression and distribution of FcRL4 and BCR in Ramos cells. Ramos cells were transfected with FcRL4-YFP and cells stably expressing FcRL4-YFP were selected. (A) FcRL4⁻ and FcRL4⁺ cells were labeled with APC-conjugated mAb specific for the human IgM (anti-IgM–APC) and PE-conjugated mAb specific for the FcRL4 (anti-FcRL4–PE) and the cell-surface expression of IgM and FcRL4 was quantified by flow cytometry. (B) The distribution of FcRL4-YFP and Fab anti-IgM–DyLight649 labeled BCR in resting cells is shown as pseudo-color epifluorescence images of FcRL4-YFP (green), BCR (red), and bright field transmitted and merged images. Images were acquired on an Olympus IX-81 microscope equipped with 100 × 1.45 numerical aperture objectives lens as described in "Preparation of PLBs and live cell imaging." The yellow scale bars represent 10 μm. Pixel intensities of FcRL4-YFP (green) and the BCR (red) in the direction by the white arrow are shown in a representative cell.

time-lapse imaging of FcRL4⁺ B cells, the FcRL4 and the BCR were co-localized at the initial points of contact of the B cell with the bilayer and continued to be co-localized through the first 100 seconds of contact (Figure 2C-D and supplemental Video 4). The BCR and FcRL4 were co-localized, although the FcRL4 was not co-ligated to the BCR. Strikingly, as IS formation continued, the BCR and FcRL4 segregated and the co-localization coefficient dropped significantly (Figure 2D). The FcRL4 perturbed normal IS formation and was concentrated in the center of the IS (supplemental Video 3), displacing the BCR to the periphery (Figure 2C and supplemental Video 4). As described in "Inhibitory function of FcRL4 requires all 3 tyrosines in its cytoplasmic tail," the inhibitory function of FcRL4 is dependent on the 3 tyrosines in the ITIM and the switch motif in the cytoplasmic domain of FcRL4. In cells expressing FcRL4 in which all 3 cytoplasmic tyrosines were mutated to phenylalanines, FcRL4 (FFF), the BCR accumulated at the interface of the cell and the bilayer (Figure 2E-F) and IS formation proceeded normally, with the BCR concentrating in the center of the IS with a higher co-localization coefficient compared with the unmutated FcRL4 (Figure 2E-G and supplemental Figure 2).

BCR signaling is blocked in FcRL4⁺ B cells

The finding that the BCR-signaling–dependent formation of an IS was disrupted by the expression of FcRL4 lead us to directly assess BCR signaling. For biochemical analyses of BCR signaling, B cells were activated using F(ab′)$_2$ anti-IgM in solution for varying lengths of time, the cells lysed in detergent buffer, the detergent lysates immunoprecipitated with Abs to Igβ, Syk, PLC-γ2, and Vav, and the immunoprecipitates subjected to SDS-PAGE and immunoblotting probing with Abs specific for phospho-tyrosine. Immediately after BCR cross-linking, the BCR is phosphorylated on the ITAMs tyrosines in the cytoplasmic domains of the Igαβ heterodimer, a function of the Src kinase Lyn.[22] The phosphorylation of Igβ was not blocked in FcRL4⁺ cells (Figure 3A). After the phosphorylation of Igαβ by Lyn, the SH2-domain–
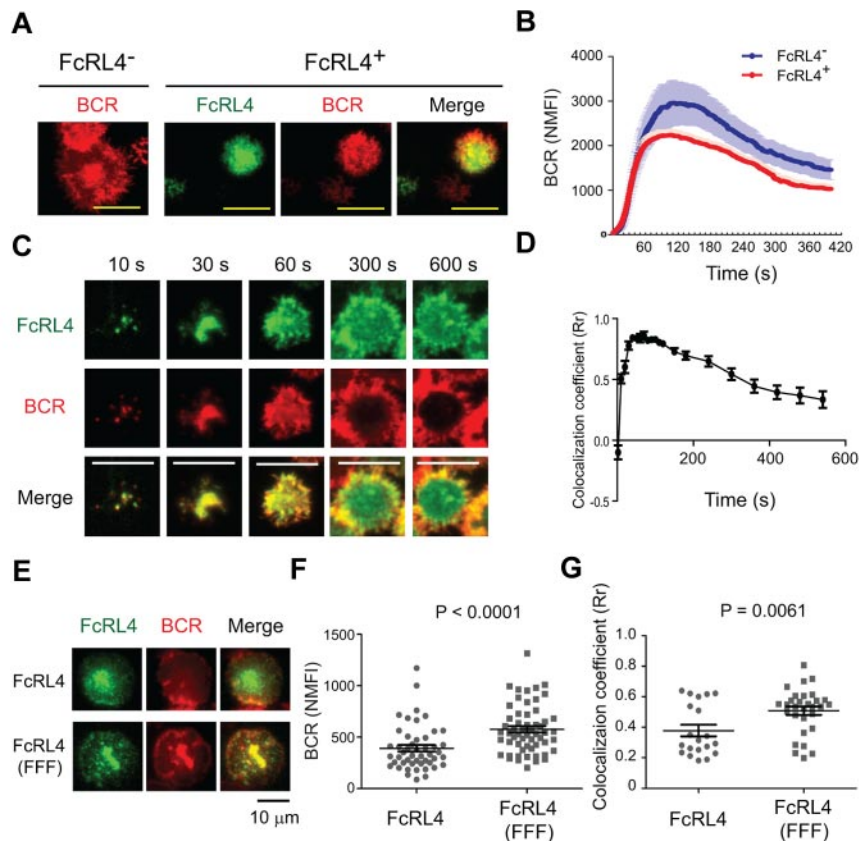
Figure 2. The spatial relationship between FcRL4 and the BCR during formation of the immune synapse. (A-D) FcRL4− B cells and FcRL4+ B cells stably expressing FcRL4-YFP were stained with Fab goat Abs specific for human IgM (Fab anti-IgM) conjugated with DyLight649 to label the BCR. The cells were placed on planar lipid bilayers containing ICAM and Fab anti-IgM at 37°C and 2-color time-lapse live cell TIRF images were recorded at 2-second intervals for 10 minutes using an Olympus IX-81 microscope equipped with a TIR illumination port, IX2 ZDC autofocus laser system, and 100 × 1.45 numerical aperture objectives lens. Images were processed as described in "Preparation of PLBs and live cell imaging" to quantify the data. (A) The distribution of the surface BCR in the contact area of FcRL4− and FcRL4+ B cells with the bilayer 5 minutes after cells contacted the bilayers. For FcRL4+ cells, images of the FcRL4 alone and merged images with BCR are given. Scale bars represent 10 μm. (B) Normalized mean fluorescence intensity (NMFI) of the surface BCR in the contact area between the cells and the bilayers with time calculated from time-lapse live-cell TIRF images are given. The mean ± SD was calculated and compared between FcRL4− (n = 18) and FcRL4+ (n = 20) B cells. (C) Dynamics of the co-localization between FcRL4 and the BCR in the contact area of FcRL4+ B cells and the planar lipid bilayer over time. Shown are FcRL4, BCR, and merged images at the indicated time points. (D) The colocalization coefficient (Rr) is given for FcRL4 and the BCR versus time calculated as mean ± SD by intensity correlation analysis between the BCR and FcRL4 in FcRL4+ cells (n = 10 from 3 different experiments). (E-G) Cells expressing either wild-type FcRL4 or all 3 tyrosines in its cytoplasmic tail-mutated FcRL4 (FFF) were labeled with both Cy3-Fab anti-IgM and Alexa Fluor 647–conjugated FcRL4-specific mAb on ice and placed on the planar lipid bilayer at 37°C. After 10 minutes of incubation on the bilayer, cells were fixed with 4% paraformaldehyde and imaged as in panel A. (E) Distribution in the contact area of the BCR (red) and either WT FcRL4 or FcRL4 (FFF; green) and merged images are shown. (F) Given are the NMFIs of the BCR in the contact area between the cells and the bilayers calculated from TIRF images for cells expressing wild-type FcRL4 (n = 50) and FcRL4 (FFF; n = 57) from the representative of 3 independent experiments. (G). Rr calculated as mean ± SD as described in panel D is given for the BCR and either wild-type FcRL4 (n = 20) or FcRL4 (FFF; n = 30).

containing kinase Syk is recruited to the phosphorylated BCR and phosphorylated.[22] In FcRL4+ B cells, Syk was phosphorylated but only transiently compared with FcRL4− B cells (Figure 3B). Using Abs specific for the phospho-tyrosine at residue 352 present in activated Syk,[23] a similar transient pattern of Syk phosphorylation was observed in FcRL4+ B cells (Figure 3C). Downstream of Syk, the phosphorylation of PLC-γ2 and Vav were decreased in FcRL4+ cells to nearly undetectable levels compared with FcRL4− B cells (Figure 3D). Calcium responses were also decreased in FcRL4+ cells compared with FcRL4− B cells (Figure 3E). In addition, the levels of expression of the activation marker CD69 were reduced in FcRL4+ cells after BCR cross-linking compared with FcRL4− cells (Figure 4A). Moreover, the decrease in the levels of BCR-cross-linking–induced CD69 expression correlated with the levels of FcRL4 expression on the B-cell surface. Comparing sorted populations of FcRL4+ cells that differed 2-fold in the levels of expression of FcRL4, higher levels of expression of FcRL4 were associated with lower levels of CD69 expression (Figure 4B). These data provide evidence that in the absence of co-ligation to the BCR,

FcRL4 blocks BCR signaling early in the cascade, namely after Igβ phosphorylation at the point of Syk phosphorylation. To determine the effect of FcRL4 expression in normal human B cells, purified human peripheral blood B cells were nucleofected with plasmids containing either YFP alone or FcRL4-YFP, and cells were incubated with medium alone or medium containing F(ab′)₂ anti-IgG + M for 18 hours, and the cells were analyzed by flow cytometry for the expression of YFP and CD69. The nucleofection process alone induced CD69 expression, but in cells expressing FcRL4, both basal and BCR-cross-linking–induced CD69 levels were reduced compared with FcRL4− cells (Figure 4C).

Inhibitory function of FcRL4 requires all 3 tyrosines in its cytoplasmic tail

FcRL4 contains 3 tyrosines in its cytoplasmic tail, 1 in a membrane proximal switch motif (Y451) and 2 in ITIM motifs (Y463 and Y493; Figure 5A). Earlier studies showed that when the tail of FcRL4 was expressed as an FcγRIIB, chimera, in a co-ligation–
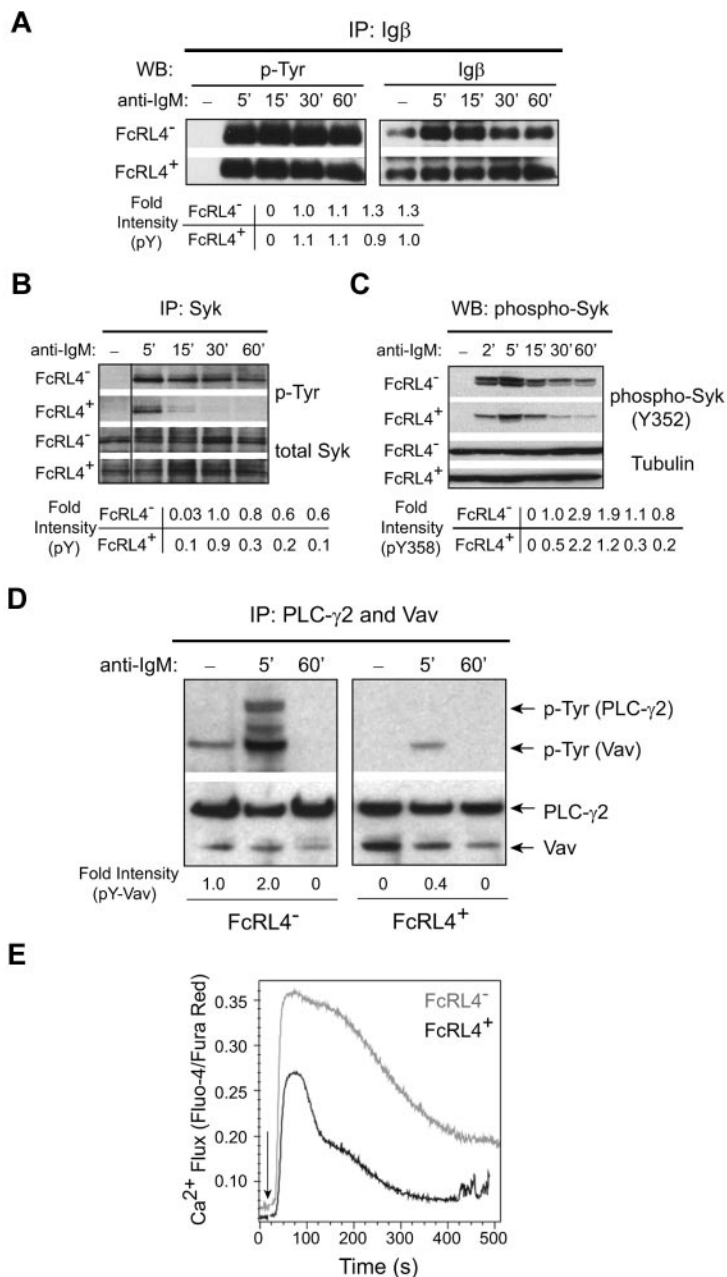
A

IP: Igβ

WB:	p-Tyr	Igβ
anti-IgM:	− 5′ 15′ 30′ 60′	− 5′ 15′ 30′ 60′

FcRL4−
FcRL4+

Fold Intensity (pY)	FcRL4−	0	1.0	1.1	1.3	1.3
	FcRL4+	0	1.1	1.1	0.9	1.0

B

IP: Syk

anti-IgM:	− 5′ 15′ 30′ 60′	
FcRL4−		p-Tyr
FcRL4+		
FcRL4−		total Syk
FcRL4+		

Fold Intensity (pY)	FcRL4−	0.03	1.0	0.8	0.6	0.6
	FcRL4+	0.1	0.9	0.3	0.2	0.1

C

WB: phospho-Syk

anti-IgM:	− 2′ 5′ 15′ 30′ 60′	
FcRL4−		phospho-Syk (Y352)
FcRL4+		
FcRL4−		Tubulin
FcRL4+		

Fold Intensity (pY358)	FcRL4−	0	1.0	2.9	1.9	1.1	0.8
	FcRL4+	0	0.5	2.2	1.2	0.3	0.2

D

IP: PLC-γ2 and Vav

anti-IgM:	− 5′ 60′	− 5′ 60′	
			← p-Tyr (PLC-γ2)
			← p-Tyr (Vav)
			← PLC-γ2
			← Vav

Fold Intensity (pY-Vav)	1.0	2.0	0	0	0.4	0

FcRL4−   FcRL4+

E

Figure 3. FcRL4 expression inhibits BCR signaling downstream of Syk. (A-B) FcRL4− and FcRL4+ B cells (1 × 10^{7}) were incubated in the absence or presence of F(ab′)$_2$ anti-IgM (10 μg/mL) for the indicated times at 37°C to cross-link the BCR and the cells were lysed in detergent buffer. The lysate was immunoprecipitated with Igβ- (A) or Syk- (B) specific Abs, and the immunoprecipitates were subjected to SDS-PAGE and immunoblotting. Immunoblots were first probed with a mAb specific for phosphotyrosine, and the blots were stripped and probed with Abs specific for either Igβ (A) or Syk (B). The phosphorylated protein (pY) immunoblots were quantified by densitometry and normalized to the total amount of Igβ or Syk. The fold intensities of at each time point relative to the pY intensity of FcRL4− cells 5 minutes after BCR cross-linking are given. Shown are representative blots of 3 independent experiments. The vertical line has been inserted to indicate a repositioned gel lane. (C) Whole-cell lysates from cells treated as in panels A and B were subjected to SDS-PAGE and immunoblotting, first with Ab specific for the phospho-tyrosine at residue 352 (pY352) of Syk and then Ab specific for tubulin. Shown is the representative of 2 independent experiments. The fold intensity of pY352 relative to pY352 of FcRL4− cells 2 minutes after BCR cross-linking is shown. (D) Cell lysates were sequentially immunoprecipitated for Vav and PLC-γ2, and both immunoprecipitates were combined and subjected to SDS-PAGE and immunoblotting, first with phospho-tyrosine–specific Abs and then with a mixture of Abs specific for Vav and PLC-γ2. The fold intensities of phospho-Vav (pY-Vav) relative to pY-Vav of FcRL4− cells 5 minutes after BCR cross-linking are given. Shown is 1 of 3 independent experiments. (E) Intracellular free Ca^{2+} was measured by flow cytometry after loading cells with Fluo-4NW and Fura Red at 37°C for 30 minutes. F(ab′)$_2$ anti-IgM was added to the cells to cross-link the BCR and data acquisition was started 30 seconds later. Fluorescence intensities of Fluo-4 and Fura Red were recorded in FL-1 and FL-3, respectively, for 512 seconds. Shown is the ratio of the fluorescence intensities of Fluo-4 to Fura Red versus time (in seconds) from 1 of 5 independent experiments. The arrow indicates the time at which the F(ab′)$_2$ anti-IgM was added to the cells.

dependent fashion the FcγRIIB-FcRL4 chimera inhibited BCR signaling. Inhibition was dependent on the tyrosines in the 2 ITIMs.[11] Each of the tyrosines in the FcRL4 tail was mutated individually to a phenylalanine (Y451F, Y463F, or Y493F) and in one construct all 3 tyrosines were mutated to phenylalanines (FFF). Ramos cells were transfected with an empty vector or constructs containing each of the mutants and cell clones with similar surface expression of FcRL4 and BCR were selected for study (supplemental Figure 3). Compared with the WT FcRL4, the FFF FcRL4 mutant's ability to block BCR-induced CD69 expression was significantly reduced (Figure 5B). Compared with cells expressing the FFF mutant, none of cells expressing single tyrosine mutants showed a significant reduction in BCR-induced CD69 expression. Cells expressing the Y493F mutation showed increased CD69 induction compared with the FFF mutant or WT FcRL4. Therefore, all 3 tyrosines in the FcRL4 tail appear to be necessary for FcRL4 inhibition of BCR signaling.

Phosphorylation of FcRL4 and recruitment of SHP-1 and SHP-2

In studies in which the tail of the FcRL4 was expressed as a chimera with the ectodomain and transmembrane domain of FcγRIIB, upon co-ligation with the BCR, the FcRL4 tail was shown to be rapidly phosphorylated and to recruit the protein phosphatases SHP-1 and SHP-2.[11] In FcRL4+ cells, FcRL4 was constitutively phosphorylated in the absence of BCR cross-linking (Figure 6A). However, BCR cross-linking resulted in an increase in FcRL4 phosphorylation at 5 minutes and then a decrease in FcRL4 phosphorylation by 30 minutes to a level of phosphorylation below that in resting cells. Therefore, in the absence of co-ligation, BCR cross-linking regulates the level of FcRL4 phosphorylation. The tyrosine phosphatase SHP-1 was associated with FcRL4 in resting cells and its association with FcRL4 was not affected by BCR cross-linking (Figure 6B). Similarly, SHP-2 was present in the immunoprecipitates of FcRL4 from resting cells, and this association did not change with BCR cross-linking (Figure 6C). FcRL4 was present in the

Figure 4. FcRL4 inhibits BCR-induced CD69 expression. (A) Several FcRL4$^-$ and FcRL4$^+$ subclones, n = 4 and n = 12, respectively, were incubated with F(ab′)$_2$ control Ig or F(ab′)$_2$ anti-IgM to cross-link the BCRs for 18-24 hours. Cells were stained with PE-coupled mAb specific for CD69 and analyzed by flow cytometry. Left panel: Representative histograms of CD69 expression on FcRL4$^-$ and FcRL4$^+$cells after treatment with control F(ab′)$_2$ or F(ab′)$_2$ anti-IgM are given. Right panel: Data shown are normalized MFI (NMFI) calculated as (MFI of positive cells × percentage of positive cells)/100 from 1 of 3 independent experiments. P values were obtained from unpaired, 2-tailed Student t test. (B) FcRL4$^+$ cells were sorted into 2 populations based on the level of FcRL4 surface expression resulting in 2-fold differences in MFI between the low- (MFI = 30) and high- (MFI = 60) expressing cells. Cells were analyzed for CD69 expression after BCR cross-linking. Left panel: Representative histogram of CD69 expression for FcRL4$^-$, FcRL4^{low} or FcRL4^{high} cells after BCR cross-linking. Right panel: NMFI of CD69 was calculated and P value obtained from unpaired, 2-tailed Student t tests either between FcRL4$^-$ and FcRL4^{low} (*P = .0134) or between FcRL4^{low} and FcRL4^{high} (**P = .0012; n = 4). (C) Purified peripheral B cells from healthy donors were nucleofected with either YFP-containing (FcRL4$^-$) or FcRL4-YFP–containing plasmids (FcRL4$^+$). After a 2-hour rest in culture, the cells were further incubated in medium alone or medium containing F(ab′)$_2$ anti-IgM + IgG for 18 hours. Cells were analyzed for CD69 expression. Left panel: Given are the representative FACS profiles of YFP and CD69 for FcRL4$^-$ or FcRL4$^+$ cells. Given are the percentages of YFP-positive or CD69-positive cells in the FcRL4$^-$ and FcRL4$^+$ populations. Right panel: NMFI of CD69 was calculated and shown by mean ± SD (n = 4). P values were obtained from paired, 2-tailed Student t tests (*P = .0124; **P = 0053).
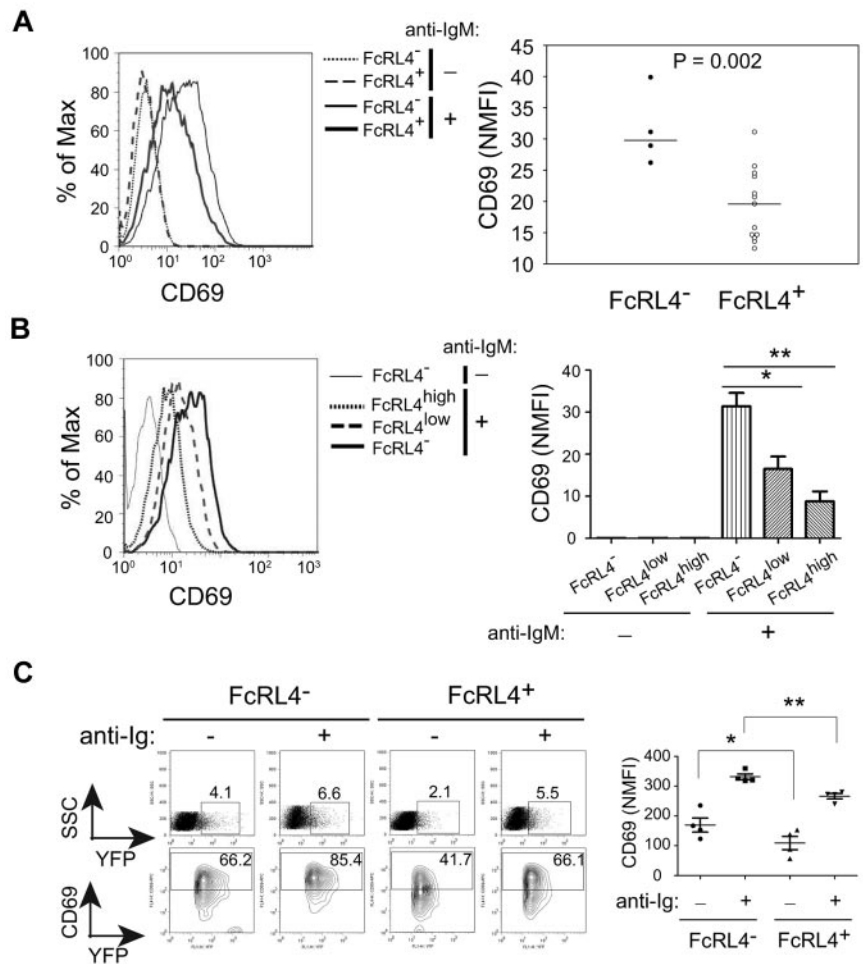
immunoprecipitates of SHP-2 from resting cells, and in cells in which the BCR was cross-linked, the amount of FcRL4 in the SHP-2 immunoprecipitate showed little change (Figure 6D).

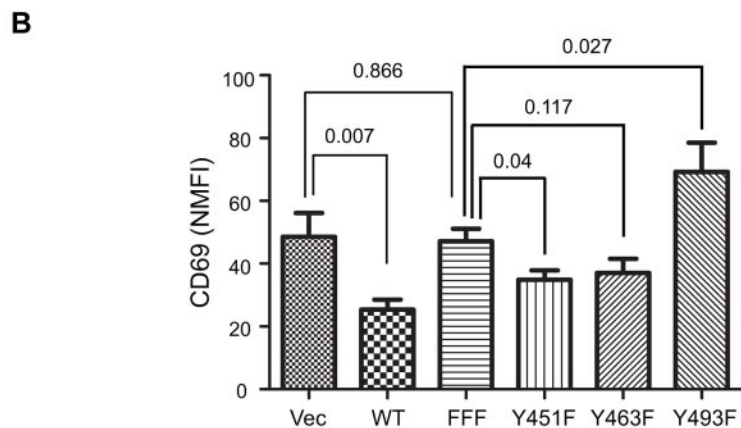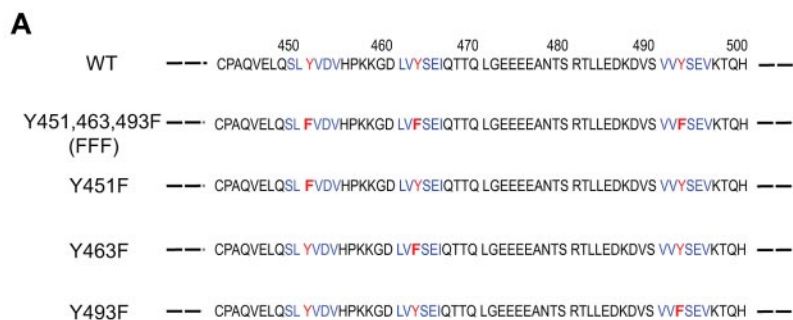### FcRL4 expression enhances TLR9 signaling

Recent studies provided evidence that ITAM- or ITIM-containing receptors have the potential to modulate TLR signaling.[24] We assessed the effect of FcRL4 expression on the response of cells to the TLR9 agonist CpG by monitoring the up-regulation of the expression of CD23 on the cell surface as an indication of TLR activation.[25] FcRL4$^-$ cells, FcRL4$^+$ cells, and cells expressing mutant FcRL4s expressed similar levels of TLR9 (supplemental Figure 4). Compared with FcRL4$^-$ cells, the response of FcRL4$^+$ cells to CpG was significantly enhanced (Figure 7A). The enhanced response to CpG was correlated with the amount of FcRL4 expressed on the cell surface (Figure 7B) and was dependent on all 3 tyrosines in the cytoplasmic tail of FcRL4 (Figure 7C), suggesting that the mechanism by which FcRL4 dampens BCR signaling and enhances TLR9 signaling may be similar. Transfection of FcRL4 into primary human B cells similarly resulted in enhanced CD23 expression in response to CpG treatment (Figure 7D). TLR9 resides in intracellular endosomal compartments in B cells, and in epifluorescence images of resting cells, we observed that a portion of FcRL4 was present in endosomal compartments (Figure 1).

Using confocal microscopy, we observed that CpG treatment resulted in the significant co-localization of FcRL4 and CpG in punctuate intracellular compartments (Figure 7E-F). This co-localization of FcRL4 and CpG suggests the possibility that FcRL4 regulates TLR9 through interactions in the endocytic compartments.

Discussion

The results presented here provide evidence that the expression of FcRL4 in B cells attenuates signaling through the BCR. Together with the recent observation in FcRL4$^+$ MBCs from HIV-viremic individuals that silencing FcRL4 increases responses to BCR cross-linking,[12] these data point to an important role of FcRL4 in regulating BCR signaling in FcRL4$^+$ MBCs. In addition, we observed that FcRL4 expression augmented CpG-induced B-cell activation through TLR9. This result suggests that FcRL4 may play a role as a molecular switch in dampening B-cell responses to antigen and enhancing innate system receptor activation in response to chronic antigen stimulation.

The molecular details of the mechanisms by which FcRL4 regulates BCR signaling and the relationship of those mechanisms to enhanced TLR9 signaling remain to be elucidated. The results presented here indicate that FcRL4 inhibition of BCR

A

B

Figure 5. All 3 tyrosines in the cytoplasmic tail of FcRL4 are necessary for its inhibitory function. (A) Amino acid sequence of the cytoplasmic domain of FcRL4, in the region containing the 3 tyrosine motifs (in blue) with the tyrosines mutated to phenylalanine in red. (B) CD69 NMFI after BCR cross-linking in cell lines stably expressing either the wild-type or mutant of FcRL4s. Data shown are from 10 independent experiments and are expressed as means ± SD. *P* values between 2 groups were obtained from unpaired, 2-tailed Student *t* test.
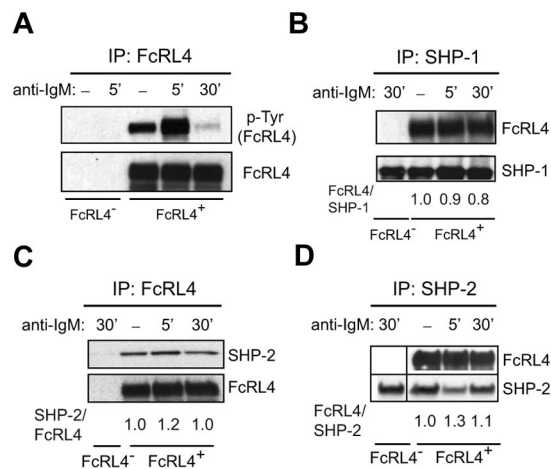
signaling targets Syk phosphorylation. By targeting Syk, FcRL4 may leave intact tonic BCR signaling necessary for B-cell survival while blocking antigen-driven BCR activation. Recent results from Rajewsky et al[26] and Alarcón et al[27] provided evidence that tonic signaling is dependent on PI3K activation and that PI3K may be recruited to the ITAMS of the BCR through the GTPase TC21. These results suggest that tonic BCR survival signaling may be independent of antigen-induced BCR signaling and would be unaffected by FcRL4 attenuation of Syk phosphorylation.

We also provide evidence that the effect of FcRL4 on BCR signaling depends on the phosphorylation of the 3 tyrosines in the cytoplasmic tail of FcRL4, and appears to be correlated with the association of the tyrosine phosphatases SHP-1 and SHP-2. SHP-1 and SHP-2 play important roles in regulating BCR signaling through their binding to the phosphorylated ITIMs of various inhibitory coreceptors.[28] SHP-1 and SHP-2 are structurally similar, having 2 adjacent amino-terminal SH2 domains, but SHP-2 has additional proline-rich sequences within its carboxy-terminal domain, and SHP-1 and SHP-2 have different affinities for the phospho-ITIM tyrosyl residues of different coreceptors,[29] suggesting similar but not identical roles in inhibition of BCR signaling. In BCR signaling, SHP-1 is recruited to a variety of ITIM-containing inhibitory coreceptors, such as CD22, CD72, ILT2, PIR-B, and LAIRs, and associates with the multiple components of proximal BCR signaling, including Lyn, Syk, BLNK, Grb2, Btk, and PLC-γ2, resulting in the down-regulation of proximal signaling events, including Syk phosphorylation, which is consistent with the results presented here. The role of SHP-2 in B-cell signaling is not yet clearly defined. SHP-2 has been reported to associate with targets such as Shc, Grb2, and the PI3K p85 subunit through the adaptor protein Gab1, suggesting distinct roles for SHP-1 and SHP-2 in the inhibition of BCR signaling.[30] Our data showed that

Figure 6. The phosphorylation of FcRL4 and its association of SHP-1 and SHP-2. FcRL4− and FcRL4+ cells (5 × 10⁷ cells) were incubated with control nonspecific F(ab′)₂ Ig or F(ab′)₂ anti-IgM to cross-link BCR for 5 or 30 minutes and the cells lysed. (A) The cell lysates were immunoprecipitated using a GFP-specific Ab to capture FcRL4-YFP. Immunoprecipitates were subjected to SDS-PAGE and immunoblotting. Immunoblots were probed with a phospho-tyrosine–specific Ab. The blots were stripped and reprobed with Abs specific for FcRL4. (B) The cell lysates were immunoprecipitated with Abs specific for SHP-1. After SDS-PAGE and immunoblotting, immunoblots were probed with Abs specific for FcRL4. The blots were stripped and reprobed with a mAb specific for SHP-1. The bands were quantified by densitometry and given are the fold intensities of FcRL4 relative to the SHP-1, with the ratio of FcRL4/SHP-1 for the control Ig cross-linking of FcRL4+ cells being 1. Each blot shown is from 1 representative experiment of 3 independent experiments. (C-D) The cell lysates were immunoprecipitated using a GFP-specific Ab and after SDS-PAGE and immunoblotting, the immunoblots were probed with Abs specific for SHP-2. The blots were stripped and probed with Ab specific for GFP (C). Alternatively, lysates were immunoprecipitated with Ab specific for SHP-2 and immunoblots were probed with Abs specific for FcRL4 (D). The blots were stripped and reprobed with Abs specific for SHP-2. Given are the fold intensities of either SHP-2 relative to the FcRL4 with the ratio of SHP-2/FcRL4 for the control Ig cross-linking of FcRL4+ cells being 1 (C) or FcRL4 relative to the SHP-2 with the ratio of FcRL4/SHP-2 for the control Ig cross-linking of FcRL4+ cells being 1 (D). In panel D, band from 30′ BCR cross-linking of FcRL4− cells was reordered from back to the front after scanning the image from the same film.
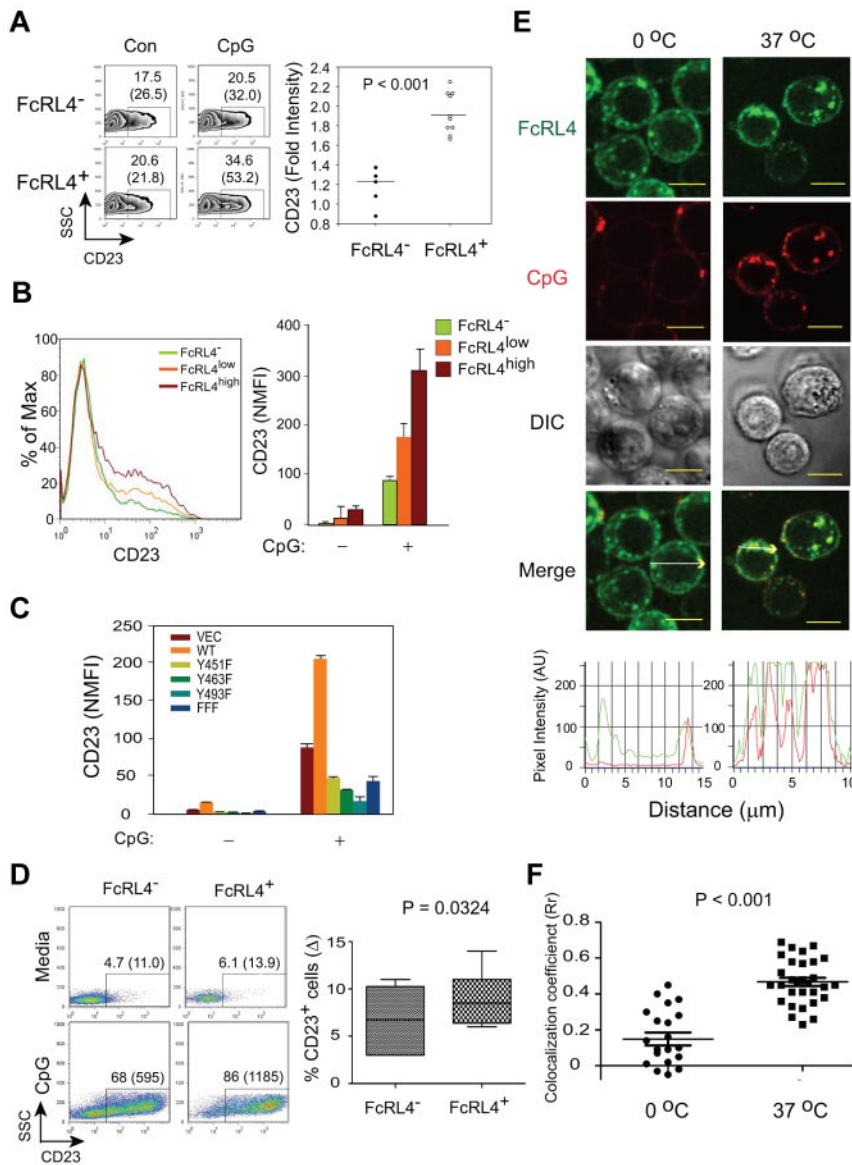
Figure 7. FcRL4 expression enhances TLR9 signaling. (A) FcRL4⁻ and FcRL4⁺ B-cell subclones were stimulated with 0.5-1.0 μM control or CpG type B 2006 ODN for 18-24 hours and analyzed for the surface expression of CD23 by flow cytometry. Left panel: Representative data for CD23 expression for FcRL4⁻ and FcRL4⁺ cells after treatment with control ODN (Con) or CpG (CpG). Given are the percentages of CD23-positive cells with mean values in parentheses. Right panel: Data shown are expressed as the fold increase in NMFIs in CpG-treated cells relative to cells treated with control ODN. P values were calculated using unpaired, 2-tailed Student t test (FcRL4⁻; n = 5; FcRL4⁺; n = 10). (B) FcRL4⁻ B cells and B cells expressing either high (FcRL4ʰⁱᵍʰ) or low (FcRL4ˡᵒʷ) levels of FcRL4 were analyzed for CD23 expression after CpG stimulation as above. Left panel: Representative histogram for CD23 expression after CpG stimulation in FcRL4⁻, FcRL4ˡᵒʷ or FcRL4ʰⁱᵍʰ cells. Right panel: NMFI of CD23 was calculated and P values obtained from unpaired, 2-tailed Student t tests either between FcRL4⁻ and FcRL4ˡᵒʷ (*P = .0358) or between FcRL4ˡᵒʷ and FcRL4ʰⁱᵍʰ (**P = .0017; n = 5). (C) B cells expressing either wild-type FcRL4, transfected with an empty vector (Vec), or expressing FcRL4 with individual tyrosine to phenylalanine mutations or all 3 tyrosine to phenylalanine mutations (Figure 5) were stimulated with CpG for 24 hours and analyzed for CD23 expression by flow cytometry. The results are expressed as NMFI. Shown is mean ± SD from 5 independent experiments. All FcRL4⁻ and FcRL4⁺ cell lines expressed similar levels of TLR9 (supplemental Figure 4). (D) Purified human B cells were nucleofected with either YFP (FcRL4⁻) or FcRL4-YFP (FcRL4⁺) plasmids and stimulated with 1.0μM CpG for 24-48 hours. Cells were analyzed for surface expression of CD23. Left panel: Representative FACS profiles for CD23 for FcRL4⁻ (YFP⁺) or FcRL4⁺ (FcRL4-YFP⁺) cells. The percentages of CD23-positive cells with the mean values in parentheses were given from the FcRL4⁻ and FcRL4⁺ populations. Right panel: The net increase of percentage of CD23-positive cells after CpG stimulation compared with the medium alone—percentage CD23⁺ cells (Δ)—was calculated within the FcRL4⁻ or FcRL4⁺ populations and shown are the means ± SD from repeated experiments with multiple donors (n = 7). P values were obtained from paired, 2-tailed Student t test. (E) FcRL4⁺ cells were stimulated with 3μM CpG-Cy3 in chambered coverglasses at 0°C or 37°C for 30 minutes, fixed, and imaged using a confocal laser scanning microscope ZEISS 510 META equipped with a 1.4 oil plan-apochromat ×63 objective lens. Two-color confocal images were acquired as described in "Preparation of PLBs and live cell imaging" and shown are pseudo-color images of FcRL4-YFP (green), CpG (red), DIC, and merged green and red images. Yellow scale bars represent 10 μm. Shown in the bottom panel are pixel intensity graphs for the FcRL4 (green) and CpG (Red) in the direction shown by the white arrows in 2 representative cells. (F) Co-localization analyses between the FcRL4 and CpG in FcRL4⁺ cells after CpG stimulation in panel E as described in "Preparation of PLBs and live cell imaging." Shown is the mean ± SD of Rr taken in single cells. P values were calculated using paired Student t test from multiple cells treated at 0°C (n = 20, ●) or at 37°C (n = 30, ■).

both SHP-1 and SHP-2 are constitutively associated with FcRL4 in resting cells and that the association was not affected by BCR cross-linking. It will be of interest to define the targets of SHP-1 and SHP-2 in FcRL4-expressing B cells and the role of both phosphatases in the inhibition of BCR signaling and the enhancement of TLR signaling.

The requirements for FcRL4 inhibition of BCR signaling described here are similar to those determined by Ehrhardt et al for

the inhibition of BCR signaling by FcRL4-FcγRIIB chimeric proteins co-ligated to the BCR.[11] An important difference between the studies in terms of the mechanism of inhibition was the requirement in their studies for BCR-FcRL4-FcγRIIB co-ligation for inhibition not observed here. Although co-ligation of the BCR and B-cell coreceptors is a common mechanism to allow coreceptor regulation of BCR signaling, for example, in the case of FcγRIIB's inhibition of BCR signaling,[31] several B-cell coreceptors regulate BCR signaling in the absence of physical co-ligation. For example, CD19, a potent enhancer of BCR signaling, is phosphorylated on BCR cross-linking, and CD19 was recently shown to co-localize with BCRs in antigen-driven BCR clusters and to be necessary for proper signaling from these clusters, all in the absence of co-ligation.[32] The transmembrane segment of FcRL4, which was replaced by the transmembrane domain of FcγRIIB in the FcRL4-FcγRIIB chimera studied by Ehrhardt et al,[11] is hydrophobic and uncharged and may facilitate its recruitment to the specialized lipid raft membrane microenvironments of the BCR clusters in the absence of co-ligation.[13] Consistent with this possibility, we showed here that in the absence of co-ligation, the FcRL4 co-localized with the BCR at the initial contact points between the BCR and an antigen-containing bilayer, a point that involves the coalescing of raft lipids around the BCR.[13]

We show here that the expression of FcRL4 simultaneously dampens BCR signaling while enhancing TLR9 signaling. FcRL4 did not appear to alter responses to T-cell help, because we observed no differences in the response to CD40 ligation or to IL-4 in FcRL4+ and FcRL4− cells (data not shown). One implication of this finding is that the ITAM-containing BCR may constitutively regulate TLR9 signaling and that, once BCR signaling is attenuated by FcRL4 expression, TLR9 may be relieved from this BCR regulation. Alternatively, FcRL4 could directly influence TLR9 signaling. There is growing evidence for the regulation of TLR signaling by ITAM-associated receptors, and it has been proposed that integration of ITAM signaling with TLR signaling may fine-tune cellular responses to extracellular stimuli.[24] Antigens that contain TLR9 agonist and have the potential to engage both the BCR and TLR9 have been shown to enhance signaling to NF-κB, a point at which the BCR and TLR9 signaling pathways intersect.[33,34] We recently provided evidence that antigen-induced BCR signaling resulted in recruitment of TLR9 from endosomes to autophagosome-like compartments into which BCRs trafficked.[35] The presence of BCRs and TLR9 in these intracellular compartments resulted in hyperactivation of MAPKs. Our finding that disruption of BCR signaling at the level of Syk influences TLR9 signaling suggest that these 2 receptors may be talking to one another through signaling pathways that proceed MAP kinases and NF-κB activation. Indeed, there is evidence that Syk-dependent activation of CARD9 and RIP2-dependent TLR activation of CARD9 upstream of MAPKs[36] may be a point of cross-talk. It will be of interest to pinpoint where this conversation occurs. Although the molecular mechanisms that underlie the observed synergistic signaling remain to be determined, the observations reported here are important for providing further evidence for cross-talk between the adaptive and innate immune system receptors.

We do not yet know what cells are precursors of FcRL4+ MBCs or what drives the differentiation of FcRL4+ MBCs. FcRL4+ MBCs were first identified in lymphoid tissues of the mucosal immune system in close proximity to sites of invading pathogens,[3] and subsequently in the peripheral blood of HIV-infected viremic individuals[5] and children and adults chronically reinfected with *P falciparum* malaria.[10] These observations suggest the possibility that continuous antigenic stimulation through the BCR may drive the differentiation of FcRL4+ MBCs. Consistent with this possibility is the finding that in HIV-infected viremic individuals, HIV-specific B cells were enriched in the FcRL4+ MBC population, in contrast to influenza-specific B cells, which were enriched in the classic MBC population.[5] We observed larger numbers of FcRL4+ MBCs in individuals with chronic asymptomatic *P falciparum* infections compared with those who cleared infections again, suggesting a role for chronic antigen exposure in the differentiation of FcRL4+ MBCs in malaria.[10] However, the relationship between antigen exposure during infections and the differentiation of FcRL4+ MBCs will remain highly speculative until we gain a better understanding of the antigen specificity of FcRL4+ MBCs and the nature of the precursors of FcRL4+ MBCs, including the relationship between FcRL4− and FcRL4+ MBCs.

In summary, we provide evidence that the expression of FcRL4, which marks a distinct population of MBCs, is sufficient to dampen BCR signaling and to enhance TLR9 signaling. Because FcRL4+ MBCs are associated with 2 chronic infectious diseases, AIDS and malaria, these findings suggest that chronic exposure to antigen may result in a switch in a population of B cells from adaptive to innate sensing cells.

Acknowledgments

Authorship

Contribution: H.W.S., R.S.D., and S.K.P. designed the research; H.W.S. and P.D.K. performed the research; R.S.D. contributed new reagents; and H.W.S. and S.K.P. analyzed the data and wrote the manuscript.

Conflict-of-interest disclosure: The authors declare no competing financial interests.

The current affiliation for P.D.K. is Beirne B. Carter Center for Immunology Research, Department of Microbiology, University of Virginia, Charlottesville, VA.

Correspondence: Susan K. Pierce, NIAID/NIH/Twinbrook II, 12441 Parklawn Dr, Rm 200B, MSC 8180, Rockville, MD 20852; e-mail: spierce@nih.gov.

References

1. Davis RS. Fc receptor-like molecules. *Annu Rev Immunol.* 2007;25:525-560.

2. Schreeder DM, Cannon JP, Wu J, Li R, Shakhmatov MA, Davis RS. Cutting edge: FcR-like 6 is an MHC class II receptor. *J Immunol.* 2010;185(1):23-27.

3. Ehrhardt GR, Hsu JT, Gartland L, et al. Expression of the immunoregulatory molecule FcRH4 defines a distinctive tissue-based population of memory B cells. *J Exp Med.* 2005;202(6):783-791.

4. Ehrhardt GR, Hijikata A, Kitamura H, Ohara O,

Wang JY, Cooper MD. Discriminating gene expression profiles of memory B cell subpopulations. *J Exp Med.* 2008;205(8):1807-1817.

5. Moir S, Ho J, Malaspina A, et al. Evidence for HIV-associated B cell exhaustion in a dysfunctional memory B cell compartment in HIV-infected viremic individuals. *J Exp Med.* 2008;205(8): 1797-1805.

6. Wherry EJ, Ha SJ, Kaech SM, et al. Molecular signature of CD8+ T cell exhaustion during chronic viral infection. *Immunity.* 2007;27(4):670-684.

7. Day CL, Kaufmann DE, Kiepiela P, et al. PD-1 expression on HIV-specific T cells is associated with T-cell exhaustion and disease progression. *Nature.* 2006;443(7109):350-354.

8. Trautmann L, Janbazian L, Chomont N, et al. Up-regulation of PD-1 expression on HIV-specific CD8+ T cells leads to reversible immune dysfunction. *Nat Med.* 2006;12(10):1198-1202.

9. Moir S, Fauci AS. B cells in HIV infection and disease. *Nat Rev Immunol.* 2009;9(4):235-245.

10. Weiss GE, Crompton PD, Li S, et al. Atypical memory B cells are greatly expanded in individuals living in a malaria-endemic area. *J Immunol.* 2009;183(3):2176-2182.

11. Ehrhardt GR, Davis RS, Hsu JT, Leu CM, Ehrhardt A, Cooper MD. The inhibitory potential of Fc receptor homolog 4 on memory B cells. *Proc Natl Acad Sci U S A.* 2003;100(23):13489-13494.

12. Kardava L, Moir S, Wang W, et al. Attenuation of HIV-associated human B cell exhaustion by siRNA downregulation of inhibitory receptors. *J Clin Invest.* 2011;121(7):2614.

13. Sohn HW, Tolar P, Pierce SK. Membrane heterogeneities in the formation of B cell receptor-Lyn kinase microclusters and the immune synapse. *J Cell Biol.* 2008;182(2):367-379.

14. Liu W, Won Sohn H, Tolar P, Meckel T, Pierce SK. Antigen-induced oligomerization of the B cell receptor is an early target of FcγRIIB inhibition. *J Immunol.* 2010;184(4):1977-1989.

15. Tolar P, Hanna J, Krueger PD, Pierce SK. The constant region of the membrane immunoglobulin mediates B cell-receptor clustering and signaling in response to membrane antigens. *Immunity.* 2009;30(1):44-55.

16. Alisi A, Giannini C, Spaziani A, Caini P, Zignego AL, Balsano C. Involvement of PI3K in HCV-related lymphoproliferative disorders. *J Cell Physiol.* 2008;214(2):396-404.

17. Sohn HW, Tolar P, Brzostowski J, Pierce SK. A method for analyzing protein-protein interactions in the plasma membrane of live B cells by fluorescence resonance energy transfer imaging as acquired by total internal reflection fluorescence microscopy. *Methods Mol Biol.* 2010;591:159-183.

18. Liu W, Meckel T, Tolar P, Sohn HW, Pierce SK. Antigen affinity discrimination is an intrinsic function of the B cell receptor. *J Exp Med.* 2010; 207(5):1095-1111.

19. Sohn HW, Gu H, Pierce SK. Cbl-b negatively regulates BCR signaling in mature B cells through ubiquitination of the tyrosine kinase Syk. *J Exp Med.* 2003;197:1511-1524.

20. Cheng PC, Dykstra ML, Mitchell RN, Pierce SK. A role for lipid rafts in B cell antigen receptor signaling and antigen targeting. *J Exp Med.* 1999; 190(11):1549-1560.

21. Cherukuri A, Carter RH, Brooks S, et al. B cell signaling is regulated by induced palmitoylation of CD81. *J Biol Chem.* 2004;279(30):31973-31982.

22. Dal Porto JM, Gauld SB, Merrell KT, Mills D, Pugh-Bernard AE, Cambier J. B cell antigen receptor signaling 101. *Mol Immunol.* 2004;41(6-7): 599-613.

23. Kulathu Y, Grothe G, Reth M. Autoinhibition and adapter function of Syk. *Immunol Rev.* 2009; 232(1):286-299.

24. Ivashkiv LB. Cross-regulation of signaling by ITAM-associated receptors. *Nat Immunol.* 2009; 10(4):340-347.

25. Hanten JA, Vasilakos JP, Riter CL, et al. Comparison of human B cell activation by TLR7 and TLR9 agonists. *BMC Immunol.* 2008;9:39.

26. Srinivasan L, Sasaki Y, Calado DP, et al. PI3 kinase signals BCR-dependent mature B cell survival. *Cell.* 2009;139(3):573-586.

27. Delgado P, Cubelos B, Calleja E, et al. Essential function for the GTPase TC21 in homeostatic antigen receptor signaling. *Nat Immunol.* 2009; 10(8):880-888.

28. Tamir I, Dal Porto JM, Cambier JC. Cytoplasmic protein tyrosine phosphatases SHP-1 and SHP-2: regulators of B cell signal transduction. *Curr Opin Immunol.* 2000;12(3):307-315.

29. Bruhns P, Marchetti P, Fridman WH, Vivier E, Daeron M. Differential roles of N- and C-terminal immunoreceptor tyrosine-based inhibition motifs during inhibition of cell activation by killer cell inhibitory receptors. *J Immunol.* 1999;162(6):3168-3175.

30. Ingham RJ, Holgado-Madruga M, Siu C, Wong AJ, Gold MR. The Gab1 protein is a docking site for multiple proteins involved in signaling by the B cell antigen receptor. *J Biol Chem.* 1998;273(46): 30630-30637.

31. Ravetch JV, Bolland S. IgG Fc receptors. *Annu Rev Immunol.* 2001;19:275-290.

32. Depoil D, Fleire S, Treanor BL, et al. CD19 is essential for B cell activation by promoting B cell receptor-antigen microcluster formation in response to membrane-bound ligand. *Nat Immunol.* 2008;9(1):63-72.

33. Yi AK, Yoon JG, Krieg AM. Convergence of CpG DNA- and BCR-mediated signals at the c-Jun N-terminal kinase and NF-kappaB activation pathways: regulation by mitogen-activated protein kinases. *Int Immunol.* 2003;15(5):577-591.

34. Leadbetter EA, Rifkin IR, Hohlbaum AM, Beaudette BC, Shlomchik MJ, Marshak-Rothstein A. Chromatin-IgG complexes activate B cells by dual engagement of IgM and Toll-like receptors. *Nature.* 2002;416(6881):603-607.

35. Chaturvedi A, Dorward D, Pierce SK. The B cell receptor governs the subcellular location of Toll-like receptor 9 leading to hyperresponses to DNA-containing antigens. *Immunity.* 2008;28(6): 799-809.

36. Mócsai A, Ruland J, Tybulewicz VL. The SYK tyrosine kinase: a crucial player in diverse biological functions. *Nat Rev Immunol.* 2010;10(6):387-402.